Quaternary river incision in NE Ardennes (Belgium) – Insights from 10Be/26Al dating of river terraces.

Article *in* Quaternary Geochronology · January 2011

CITATIONS
11

READS
60

6 authors, including:

Gilles Rixhon
University of Cologne
31 PUBLICATIONS **158** CITATIONS
SEE PROFILE

Didier L Bourlès
Aix-Marseille Université
487 PUBLICATIONS **7,567** CITATIONS
SEE PROFILE

Lionel Louis Siame
Aix-Marseille Université
105 PUBLICATIONS **1,433** CITATIONS
SEE PROFILE

Alain Demoulin
University of Liège
83 PUBLICATIONS **918** CITATIONS
SEE PROFILE

Quaternary Geochronology 6 (2011) 273–284

Contents lists available at ScienceDirect

Quaternary Geochronology

journal homepage: www.elsevier.com/locate/quageo

Research Paper

Quaternary river incision in NE Ardennes (Belgium)—Insights from $^{10}Be/^{26}Al$ dating of river terraces

Gilles Rixhon [a,b,*], Régis Braucher [c], Didier Bourlès [c], Lionel Siame [c], Benoît Bovy [a,b], Alain Demoulin [a,b]

[a] Department of Physical Geography and Quaternary, University of Liège, Belgium
[b] Fund for Scientific Research – FNRS, Brussels, Belgium
[c] CEREGE, Univ. Aix-Marseille III, France

ARTICLE INFO

Article history:
Received 18 March 2010
Received in revised form
22 October 2010
Accepted 5 November 2010
Available online 12 November 2010

Keywords:
Cosmogenic nuclides
River incision
River terrace dating
Geomorphology
Rhenish shield
Ardennes massif

ABSTRACT

Although it constitutes a main tool to unravel the regional recent tectonics, the chronology of the Pleistocene river incision is still poorly constrained within the uplifted Ardennes massif (Western Europe). Here, we use *in situ* produced cosmogenic ^{10}Be and ^{26}Al concentrations from depth profiles in terrace sediments of several Ardennian rivers (Meuse, Ourthe and Amblève) in order to date the so-called Younger Main Terrace (YMT), a key-level in the drainage network evolution. We present the first absolute dating of the YMT in the lower Meuse valley, where we obtained an age of 725 ± 120 ka for a terrace deposit buried beneath 3 m of Weichselian loess at Romont. This age is consistent with some previously published estimates based on paleomagnetic data and MIS correlations. However, the ages we obtain for the same terrace level in Ardennian tributaries of the Meuse are significantly younger: 390 ± 35 ka in the lower Ourthe, and only 220 ± 31 ka still farther upstream, in the lower Amblève. We thus demonstrate that the post-YMT incision occurred diachronically in NE Ardennes. The ~0.5 Ma timespan needed by the erosion wave to propagate from the lower Meuse towards the Ardennian headwaters contradicts the long-held statement of a climatically driven incision that would have been synchronous throughout the catchments. Finally, we interpret the strong ^{10}Be enrichment displayed by the lower half of the Belle–Roche (lower Amblève) profile as betraying the long-lasting, slow accumulation of the ~8 m thick terrace deposit in that place.

1. Introduction

River terraces constitute the main tool to constrain river incision, triggered either by climatic fluctuations or by tectonic activity at a regional scale. In NW Europe, terrace sequences have been largely correlated to Quaternary climatic variations (Antoine, 1994; Cordier et al., 2006; Bridgland and Westaway, 2008) but, at the same time, have been widely used as an indicator of tectonic uplift (Maddy, 1997; Westaway, 2002; Westaway et al., 2006). Recent reviews on the interfering influences of tectonics, climate and eustatism on river evolution have been given by Antoine et al. (2000) and Bridgland (2000).

While geodetic estimates of the present-day uplift rate of the Rhenish shield are surprisingly high (Mälzer et al., 1983; Demoulin, 2004), long term rate estimates as well as the timing of uplift suffer from largely unverified assumptions. The terrace sequences of the main rivers crossing the massif (Rhine, Meuse and Mosel) have long been used to infer tectonic uplift (Brunnacker and Boenigk, 1983; Van Den Berg and Van Hoof, 2001; Westaway, 2002), but the scarcity of reliable chronological data, and especially of absolute ages, remains problematic. Indeed, while uplift rate and amount have been derived from river incision since the abandonment of the Main Terrace level of these rivers (Meyer and Stets, 1998; Van Balen et al., 2000), the age of this level relies only on diversely interpreted paleomagnetic data in the Rhine and Meuse valleys (Felder and Bosch, 1989; Van Den Berg, 1996; Boenigk and Frechen, 2006). Moreover, age data for the main intra-massif tributaries of the Rhine and the Meuse are very scarce and limited to the last ~200 ka (e.g., Cordier et al., 2006).

Within this general context, insufficient chronological constraints essentially come from the difficulty to obtain numerical ages for middle Pleistocene river terraces using conventional dating methods. To overcome this difficulty, we use here the Cosmic Ray Exposure (CRE) method, a technique that has drastically progressed during the last two decades (e.g., Nishiizumi et al., 1989; Gosse and Phillips, 2001; Granger and Muzikar, 2001). Although CRE dating has been successfully used to determine the age of surficial deposits

* Corresponding author. Department of Physical Geography and Quaternary, University of Liège, Allée du 6-Aout, 2, 4000 Liege, Belgium. Tel. +32 43665255.
E-mail address: Gilles.Rixhon@ulg.ac.be (G. Rixhon).

1871-1014/$ – see front matter © 2010 Elsevier B.V. All rights reserved.
doi:10.1016/j.quageo.2010.11.001

(e.g., glacial deposits, alluvial fans) and has already been applied to terrace material (Brocard et al., 2003; Siame et al., 2004), dating old (several hundreds of ka) river terraces remains highly difficult because of the various processes (inheritance, post-depositional erosion and/or burial) potentially perturbing the cosmogenic nuclide (TCN) production at the terrace site.

In this study, we use a profiling technique to measure the ^{10}Be and ^{26}Al concentrations at depths along five thick gravel deposit sequences of the well-preserved Main Terrace levels in the Meuse catchments. Aimed to put constraints on the history of the middle Pleistocene uplift/incision episode in the Rhenish shield, the ating of the Main Terrace level in different places from the lower Meuse in the Maastricht area through tributary and sub-tributary upstream towards its Ardennian headwaters. It will thus also contribute to enlarge the data set required to explore the spatio-temporal characteristics of the mechanism by which river incision responded to combined tectonic and climatic signals.

2. Study area

2.1. Geological setting

Located to the east of the Lower Rhine Embayment (northern-most segment of the European Cenozoic Rift System - ECRS, Fig. 1A), the Ardennes represents the western prolongation of the Paleozoic Rhenish Shield. Encompassing the study area, the NE Ardennes is mainly composed of the Caledonian Stavelot massif, whose complex folded and faulted structures emerge from the surrounding Variscan Ardennes anticlinorium and deform slightly metamorphosed slates and quartzites. To the northwest, the Dinant synclinorium exposes mainly Upper Devonian psammites and Carboniferous limestones.

As a part of the Rhenish Shield, the Ardennes experienced a moderate late Cenozoic tectonic uplift in response either to compressive stresses (lithospheric buckling) exerted by the Alpine belt on its foreland (Ziegler et al., 1995; Ziegler and Dezes, 2007) or to mantle upwelling beneath the nearby Eifel area (Ritter et al., 2001). Since the late Oligocene, the NE Ardennes would have been uplifted by 400–500 m (Demoulin, 1995). The uplift rate increased a first time at the Pliocene–Pleistocene transition and again sometime at the beginning of the middle Pleistocene. This last uplift episode raised the Ardennes by 100–200 m (Demoulin and Hallot, 2009), inducing a wave of backward erosion within the Ardennian river network (Demoulin et al., 2009).

2.2. The Younger Main Terrace (YMT)

The study area comprises the lower Meuse reach between Liège and Maastricht, the main tributary of the Meuse in the north-eastern Ardennes, called the Ourthe (drainage area ~3600 km^2) and a sub-tributary, the Amblève (drainage area ~1100 km^2) (Fig. 1B). Although the terrace flight is fairly different between the lower Meuse (23–31 levels according respectively to Juvigne and Renard, 1992 and Van Den Berg and Van Hoof, 2001) and the lower reaches of its two tributaries (19 levels for the Ourthe (Cornet, 1995) and 11 levels for the Amblève (Rixhon and Demoulin, 2010)), the so-called Main Terrace complex is well-preserved in the three valleys, where it represents a more or less continuous geomorphic marker. Mainly composed of extended terrace remnants, this complex consists generally of three closely spaced

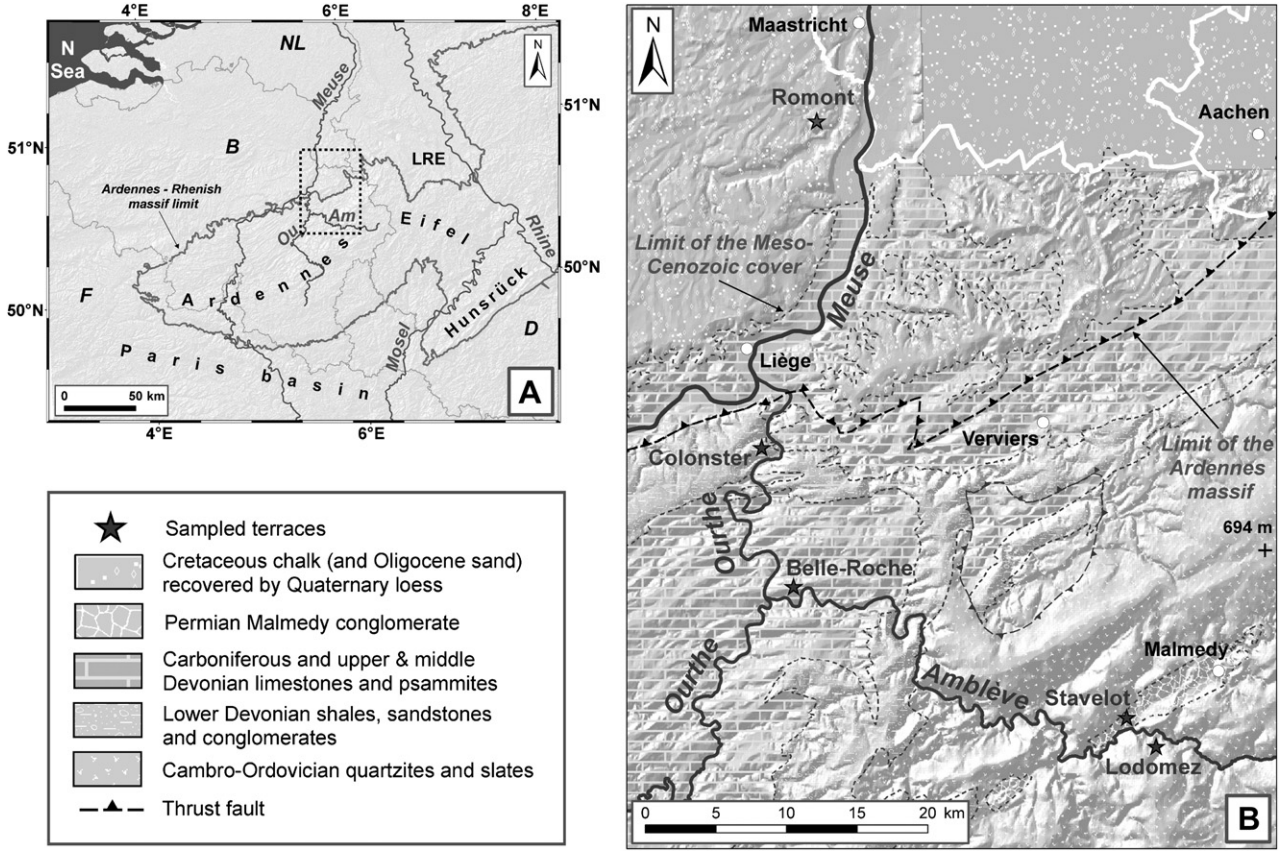

Fig. 1. A. Localization of the study area within the Rhenish shield (western Europe) (B: Belgium; F: France; D: Germany; NL: Netherlands; LRE: Lower Rhine Embayment. *Am* and *Ou* refer respectively to the Amblève and Ourthe rivers. B. Simplified geological map of the study area and localization of the sampling sites.

alluvial levels, whose elevation above the current floodplain decreases upstream, from ~65 m in the lower Meuse to ~50 m in the lower Amblève. Morphologically, it marks a sharp transition in the transverse profile of the main Ardennian valleys between a broad, gently sloping Early Pleistocene valley characterized by wide terrace surfaces and a nested narrow Middle Pleistocene valley with steeper slopes and more confined and scarcer terraces (Meyer and Stets, 1998; Van Balen et al., 2000; Houtgast et al., 2002, see Fig. 2). As the youngest level of this Main Terrace complex is directly located at the edge of the incised valley (Fig. 2), it is often used as a reference level to identify the start of the middle Pleistocene uplift/incision episode (Meyer and Stets, 1998; Van Balen et al., 2000).

3. CRE dating of river terraces

3.1. Theoretical background

Inelastic interactions of the primary cosmic ray particles (essentially protons and α particles) reaching the Earth's environment with nuclei of the atoms constituting the atmosphere produce a cascade of reactions and of energetic secondary particles (mainly neutrons and muons). The atmospheric cosmogenic nuclide species, such as ^{14}C or ^{10}Be, are the residues of the nuclear reactions induced in the atmosphere by both primary and secondary particles. Although most of their net energy is lost to the atmosphere, some of the secondary particles reach the Earth's surface with enough energy to induce nuclear reactions with lithospheric nuclei targets (^{16}O, ^{27}Al, ^{28}Si, ^{40}Ca, ^{56}Fe…) and to produce *in situ* cosmogenic nuclide species. Because interaction with matter reduces the cosmic ray flux with a characteristic exponential attenuation length, the cosmogenic nuclide production rates decrease approximately exponentially with the mass of overlying material (Gosse and Phillips, 2001).

In the Earth's crust, the evolution of an *in situ* cosmogenic nuclide production rate $P(x)$ as a function of depth (x, *expressed in g/cm²*) is commonly described by

$$P(x) = P_0 e^{(-x/\Lambda)} \quad (1)$$

where P_0 is the surface production rate (in atom/g/yr) and Λ is the attenuation length (g/cm²). Three main types of secondary particles are involved in the *in situ* production of cosmogenic nuclides: fast nucleons (essentially neutrons), stopping (or negative) muons and fast muons. Each of them has its own effective attenuation length. While the fast neutron attenuation length of 160 g/cm² is no longer debated (Lal, 1991; Brown et al., 1995), we used for the muonic attenuation lengths the values proposed by Braucher et al. (2003), i.e., 1500 g/cm² for stopping muons and 5300 g/cm² for fast muons. It has been shown that the combined use of the fast nucleon and muon contributions along a depth profile using a single cosmogenic nuclide allows assessing simultaneously the exposure time and the denudation rate of a landform (Siame et al., 2004; Braucher et al., 2009).

Assuming that the studied material experienced a single cosmic ray exposure episode and that the production and erosion rates remained constant through time, the *in situ*-production of ^{10}Be is given by the following equation:

$$C_{(x,\varepsilon,t)} = \frac{P_n}{\frac{\varepsilon}{\Lambda_n}+\lambda}\cdot e^{-\frac{x}{\Lambda_n}}\left[1-\exp\left\{-t\left(\frac{\varepsilon}{\Lambda_n}+\lambda\right)\right\}\right] + \frac{P_{\mu s}}{\frac{\varepsilon}{\Lambda_{\mu s}}+\lambda}\cdot e^{-\frac{x}{\Lambda_{\mu s}}}\left[1-\exp\left\{-t\left(\frac{\varepsilon}{\Lambda_{\mu s}}+\lambda\right)\right\}\right] + \frac{P_{\mu f}}{\frac{\varepsilon}{\Lambda_{\mu f}}+\lambda}\cdot e^{-\frac{x}{\Lambda_{\mu f}}}\left[1-\exp\left\{-t\left(\frac{\varepsilon}{\Lambda_{\mu f}}+\lambda\right)\right\}\right] + C_0\cdot e^{(-\lambda t)} \quad (2)$$

where $C(x, \varepsilon, t)$ is the ^{10}Be concentration as a function of depth x (g/cm²), erosion rate ε (g/cm²/yr) and exposure time t (yr), λ is the radioactive decay constant (yr^{-1}), and P_n, $P_{\mu s}$ and $P_{\mu f}$ are the relative production rates due to neutrons, slow muons and fast muons assuming relative contributions to the total surface production rate of 97.85%, 1.50% and 0.65% respectively. Λ_n, $\Lambda_{\mu s}$, and $\Lambda_{\mu f}$ are the effective apparent attenuation lengths (g/cm²), for neutrons, slow muons, and fast muons, respectively (Braucher et al., 2003). Finally, C_0 is the number of atoms present at the initiation of the exposure scenario (i.e., inheritance).

3.2. Sampling sites

The search for adequate sampling sites was determined by two main constraints. Firstly, as we expected that the material to be dated was older than 0.5 Ma, the need for including the muonic component in the analysis required the sampling of depth profiles in deposits deeper than 3 m below the surface. Secondly, in order to reduce problems resulting from post-depositional reworking or erosion of the terrace sediments, we selected only well-preserved terrace elements characterized by an extended (>100 m wide) even, horizontal ground surface and we sampled them in their central part. From the five sampled sites, three are located in the Amblève valley, one in the lower Ourthe and one in the lower Meuse (Fig. 1B). Except in the last valley where the sampling site was located in a quarry (*cf.* Romont site), large pits were dug in all places. Samples were collected at regular depth intervals (generally

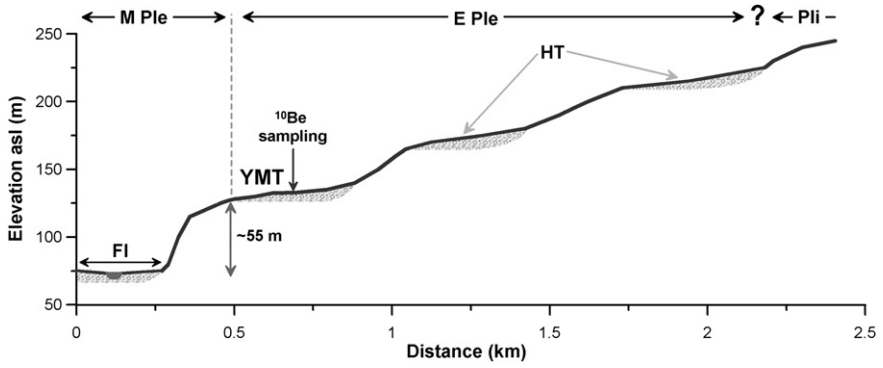

Fig. 2. Cross-section in the lower Ourthe valley at Colonster. Morphologically, the Younger Main Terrace (YMT) is located at the hinge between a broad, gently sloping Early Pleistocene valley with wide terrace surfaces (E Ple) and a narrow middle Pleistocene valley with steeper slopes and more confined and scarcer terraces (M Ple). Pli: Pliocene valley; HT: Higher Terraces; Fl: present-day floodplain.

0.5 m), a sample consisting of one large or several smaller quartz or quartzite pebbles originating from the Stavelot massif.

3.2.1. The main terrace at romont (Meuse River)

The Romont terrace is located 4 km to the west of the present Meuse channel, ~20 km to the north of the Ardennes margin (Fig. 1.B). The top of the gravel layer is situated at an elevation of ~115 m asl, and 60 m above the Meuse floodplain. According to Juvigne and Renard (1992), the Romont terrace belongs to the Hermée – St Pietersberg levels that most authors agree to recognize as forming the Main Terrace complex.

Importantly, at Romont, the 5 m thick gravel layer is nowadays overlain by 3 m of loess inherited mostly from the last glacial period, as witnessed by Weichselian paleosoils (MIS 4–2) and a tephrostratigraphic marker occurring within the loess sequence close to the sampled terrace. However, at the same site, Eemian paleosoils attesting of pre-Weichselian material at the base of the sequence have also been found in a filled paleogully where the loess thickness exceeds 10 m.

This suggests that the Romont area might have been repeatedly covered by loess during the middle Pleistocene glacials, much or all of a loess accumulation being removed during the following interglacial. In any case, the loess shielded for sometime the river gravels from exposure to the cosmic particles, so that we will have to consider the $^{26}Al/^{10}Be$ ratio in order to produce a deposition age. Six samples for ^{10}Be and ^{26}Al concentration measurements have been taken from the Romont profile (Fig. 3).

3.2.2. The main terrace at colonster (OurtheRiver)

Located in the lower Ourthe, ~9 km upstream of the Meuse confluence in Liège (Fig. 1B), the Colonster terrace has a relative elevation of 55 m above the modern floodplain (or 131 m asl) and is geometrically correlated with the YMT in the lower Meuse (Cornet, 1995). A cross-section of the Ourthe valley at Colonster remarkably illustrates the terrace location at the hinge between the older broad valleys and the younger incised one (Fig. 2).

We collected 10 samples from the ~4 m thick gravel layer covered by a thin (<1 m) alluvial silt/loess cover. The Ourthe gravels are here much coarser than those of Romont and contain boulders up to 0.5 m in diameter (Fig. 3).

3.2.3. The main terrace at belle–roche (AmblèveRiver)

Cut in Carboniferous limestones, the Belle–Roche terrace (~153 m asl) is located in the Amblève valley, 2 km upstream of the Ourthe-Amblève confluence (Fig. 1.B). Although the morphological hinge between nested valley forms is not well expressed in this reach of the Amblève, the elevation of the terrace relative to the floodplain (~53 m), similar to that of the Colonster terrace, and its great extent allow again a correlation with the YMT level (Van Balen et al., 2000; Juvigne et al., 2005; Rixhon and Demoulin, 2010).

At Belle–Roche, the river gravels appear at a depth of ~0.3 m, immediately beneath the modern soil (Fig. 3). Made of coarse pebbles within a sandy-silty matrix, the alluvial deposit is characterized by an unusually great thickness (~8 m) (Fig. 3). As pointed out by Juvigne et al. (2005), this seems unrelated with the karstic nature of the bedrock as no deformation of the river sediments is observed. We collected here 10 samples.

3.2.4. The terraces at Stavelot and Lodomez (AmblèveRiver)

Located in the upstream part of the middle Amblève valley (more than 50 km from the Ourthe confluence, Fig. 1B) and distant

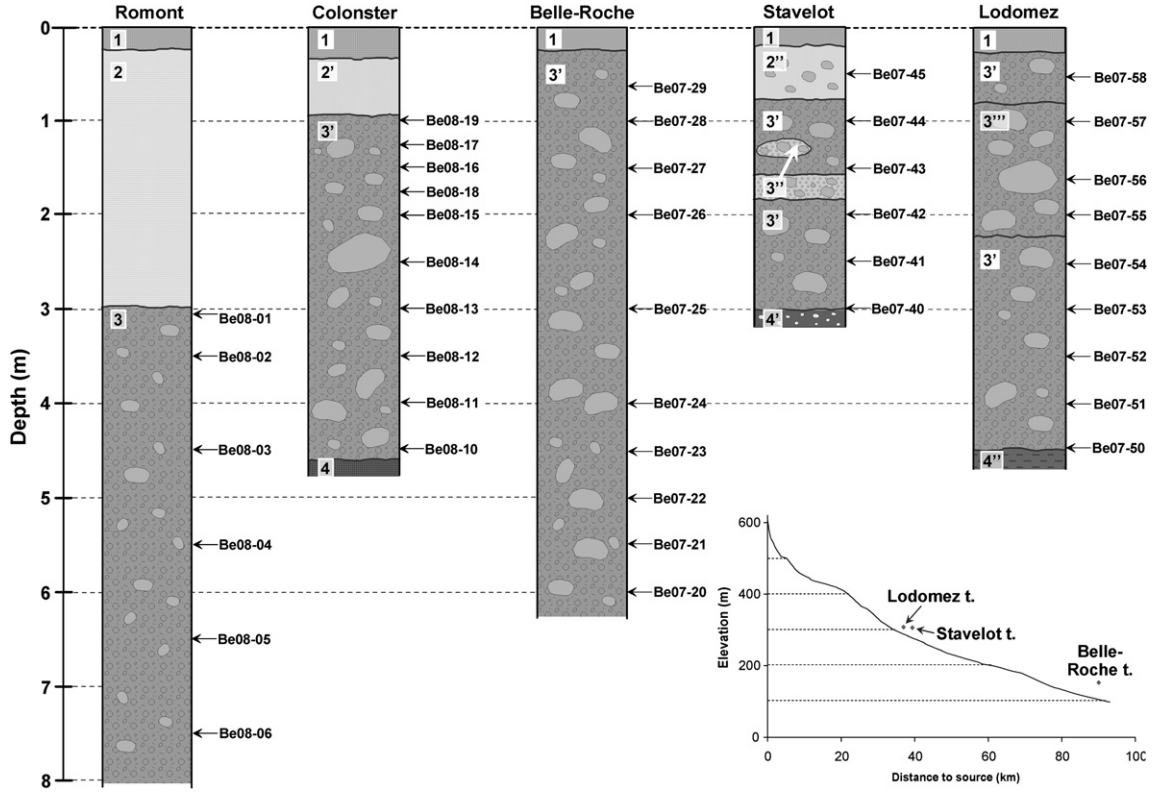

Fig. 3. Sections in the sampled terraces and Amblève long profile with localization of the sampling sites in this river. 1: modern soil; 2 & 2': loess deposits; 2'': fluvial fine matrix (loam-clay) including some pebbles; 3: fluvial gravel characterized by small-sized elements (pebbles); 3': fluvial gravel including coarser elements; 3'': fluvial lenses characterized by the lack of fine elements (sand to clay); 3''': fluvial gravel with very coarse elements (boulders); 4: shale bedrock; 4': argillite bedrock with fine conglomeratic elements; 4'': slate bedrock.

from each other by ~2.5 km, the Stavelot and Lodomez terraces are situated within the Stavelot massif (Fig. 1B). With elevations of ~305 m and ~307 m asl, the elevations of the Stavelot and Lodomez terraces relative to the local floodplain are only of ~25 m and ~20 m. Though the relative elevation of the YMT has also significantly decreased in this upstream reach of the valley, the correlation of the Stavelot and Lodomez terraces with the YMT level is problematic not only for altitudinal reasons but also because of (*i*) the convergence of all terrace levels towards a knickpoint located 12 km further upstream in the river profile, (*ii*) the damped contrast between upper broad and lower narrow valleys in this area and (*iii*) the presence of the Quarreux gorge whose increased gradient complicates the correlation between the terraces located downstream and upstream (Rixhon and Demoulin, 2010). The Stavelot and Lodomez terrace remnants likely belong to the terrace level immediately below the YMT.

Six samples have been taken from the 2.7 m thick coarse gravels of the Stavelot terrace, which are overlain by ~0.7 m of alluvial loam (Fig. 3). Nine samples have been taken from the 4.5 m thick Lodomez section, which displayed the coarsest observed river gravels ($D_{50} > 20$ cm).

4. Results

4.1. Concentration measurements and profiles

The chemical treatment of the samples and the AMS measurements were carried out at the CEREGE laboratory in Aix-en-Provence. Samples were prepared for cosmogenic nuclide concentration measurements following chemical procedures adapted from Brown et al. (1991) and Merchel and Herpers (1999). All the data reported in this study (Table 1) have been measured at ASTER (CEREGE, Aix-en-Provence). After addition in each sample of ~100 μl of an in-house 3.10^{-3} g/g ^{9}Be carrier solution prepared from deep-mined phenakite (Merchel et al., 2008), all ^{10}Be concentrations were normalized to ^{10}Be/^{9}Be SRM 4325 NIST standard with an assigned value of $(2.79 \pm 0.03)\times10^{-11}$. This standardization is equivalent to 07KNSTD within rounding error. The obtained ^{26}Al/^{27}Al ratios were calibrated against the ASTER in-house standard SM-Al-11 with ^{26}Al/^{27}Al = $(7.401 \pm 0.064)\times10^{-12}$, which has been cross-calibrated against the primary standards certified by a round-robin exercise (Merchel and Bremser, 2004) and using a ^{26}Al half-life of $(7.17 \pm 0.17)\times10^{5}$ years (Granger, 2006). ^{27}Al concentrations, naturally present in the samples, were measured at CEREGE by ICP-OES. Analytical uncertainties (reported as 1σ) include uncertainties associated with AMS counting statistics, AMS external error (0.5%), chemical blank measurement, and, regarding ^{26}Al, ^{27}Al measurement. Long term AMS measurements of chemically processed blank yield ratios on the order of $(3.0 \pm 1.5)\times10^{-15}$ for ^{10}Be/^{9}Be and $(2.2 \pm 2.0)\times10^{-15}$ for ^{26}Al/^{27}Al (Arnold et al., 2010).

Cosmocalc add-in for excel (Vermeesch, 2007) has been used to calculate sample thickness scaling (with an attenuation coefficient of 160 g cm^{-2}) and atmospheric pressures. Production rates were scaled following Stone (2000) with a sea level high latitude production rate of (4.5 ± 0.3) at/g/yr for ^{10}Be and a half-life of $(1.387 \pm 0.012)\times10^{6}$ years were used for this nuclide (Chmeleff et al., 2010; Korschinek et al., 2010). When measured against ^{26}Al KNSTD10650, the ASTER standard, which is the only available ^{26}Al standard cross-calibrated against the primary standards certified by a round-robin exercise, yields a ratio of $7.554 \pm 0.104\times10^{-12}$, 2.1% higher than the nominal value (Cronus calculator documentation, 2009, page 6). Therefore, the SM-Al-11/07KNSTD standardization we use here implies a ^{26}Al/^{10}Be production ratio of 6.61 ± 0.50. This value and its associated uncertainty are directly derived from the update of the ratio originally determined by Nishiizumi et al. (1989). They were used in all calculations and modeling for ^{26}Al.

Plotting the concentrations against sample depth provided the ^{10}Be concentration profiles from which we will model the terrace ages. A look at the ^{10}Be concentration evolution with depth reveals that the Colonster and Stavelot profiles agree rather well with the exponential decrease expected from the theory (Fig. 4), although the deepest sample at Stavelot (Be07-40, not used in the modeling) displays a surprisingly high concentration. Its ^{10}Be content is indeed more than three times higher than that of the sample just above (Table 1). This might be interpreted as a ^{10}Be accumulation prior to deposition (high ^{10}Be inheritance).

However, the lower part of the Belle–Roche profile and, to a lesser extent, that of Lodomez show a similar ^{10}Be enrichment, consistent over several samples at depths > ~500–600 g/cm^2 (Fig. 4). The inheritance hypothesis that might have explained the Be07-40 anomaly alone is hardly applicable in particular to the Belle–Roche lower profile, displaying a progressive enrichment with depth. This feature appears clearly disconnected from the exponential profile followed by the shallower (<3 m depth) samples. Note also that the well expressed exponential curve of the upper part of the profile rules out any perturbation of the latter by karstic processes in the underlying bedrock.

A similar ^{10}Be concentration anomaly is also observed in the Lodomez profile (Table 1). Though much less patent than in Belle–Roche, it might confirm that the phenomenon has more than a local meaning.

In the following modeling, we therefore consider that the concentration anomalies observed at depth >3 m in the three Amblève sites require a separate analysis and we calculate the terrace exposure times on the basis of the near-surface samples that display the expected exponential concentration decrease with depth.

4.2. Age determination

We use the Monte Carlo modeling approach developed by Braucher et al. (2009) to estimate four-parameters from the profile data, namely the terrace exposure time (t), the denudation rate (ε), the ^{10}Be inheritance and the material (i.e., alluvial deposit) density (ρ). As stated by these authors, the modeling procedure is actually very sensitive to density when one wants to determine from a ^{10}Be concentration depth profile both the exposure time and the denudation rate affecting alluvial deposits. In the present work, density was hardly measurable in the field and was likely to provide overestimated results because of the presence of numerous boulder-sized quartzitic clasts in the deposits (especially in the Ourthe and Amblève terraces, Fig. 3). As the ^{10}Be distribution with depth fairly matched the theoretically expected exponential profile, it was therefore preferable to treat density as a free parameter, like exposure time, denudation rate and inheritance (Braucher et al., 2009). Here, we let the density free to adjust within the range 1.8–2.4 g/cm^3 with an increment step of 0.1 g/cm^3. It was also assumed to be constant with depth since no particular fluvial structure was observed in the alluvial deposits (except very locally in the Stavelot terrace, Fig. 3).

The results are presented in the Table 2 with their minimum chi-square (χ^2) value (the minimum value among the medians of 100 χ^2 values issued by the Monte Carlo process for each (t,ε) pair determines the solution pair). Theoretically, a unique (t,ε) solution is found but the analytical errors and especially the modeling uncertainty frequently lead to rather large confidence intervals. Indeed, the distributions shown on the top and right sides of the plot of Fig. 5 refer only to the analytical error as propagated by the Monte Carlo procedure, to which we have to add the modeling

Table 1
Results of the $^{10}Be/^{26}Al$ analyses. Shielding factor is 1 for each terrace and the altitude refers to the top of the fluvial deposits.

Sample	Lat. (°N)	Long. (°E)	Altitude (m)	Depth (cm)	Depth (g/cm^2)	Stone scaling factor[a]	Dissolved quartz (g)	^{9}Be carrier[b] (10^{19} at.)	$^{10}Be/^{9}Be$	[^{10}Be] (10^5 at./g)	[^{10}Be] error (10^5 at./g)	[^{27}Al][c] (10^{19} at.)	$^{26}Al/^{27}Al$	[^{26}Al] (10^5 at./g)	[^{26}Al] error (10^5 at./g)
Romont terrace (*Meuse valley*)															
Be08 Ro-01	50.787	5.66	110	310	620	1.134	20.587	2.019	6.67E-13	6.544	0.104	1.043	5.08E-12	25.734	3.019
Be08 Ro-02				350	700		21.791	2.042	3.56E-13	3.339	0.080	13.004	2.50E-13	14.896	1.267
Be08 Ro-03				450	900		23.371	2.013	2.17E-13	1.869	0.052	1.953	1.10E-12	9.234	0.452
Be08 Ro-04				550	1100		21.508	2.115	1.38E-13	1.361	0.131	1.168	8.61E-13	4.677	0.400
Be08 Ro-05				650	1300		20.317	2.060	2.58E-13	2.619	0.060	1.676	1.20E-12	9.920	0.493
Be08 Ro-06				750	1500		23.404	2.071	2.19E-13	1.937	0.051	1.962	8.38E-13	7.020	0.334
Colonster terrace (*Ourthe valley*)															
Be08 Co-10	50.576	5.579	134	450	810	1.160	22.302	1.906	1.54E-13	1.316	0.077	7.156	9.97E-14	3.199	0.365
Be08 Co-11				400	720		20.950	2.038	9.33E-14	0.908	0.067	7.418	5.86E-14	2.076	0.165
Be08 Co-12				350	630		20.636	2.015	1.52E-13	1.488	0.055	1.305	8.95E-13	5.661	0.467
Be08 Co-13				300	540		21.774	2.029	1.59E-13	1.480	0.097	4.522	2.35E-13	4.880	0.263
Be08 Co-14				250	450		20.537	2.031	3.13E-13	3.095	0.112	4.970	2.70E-13	6.531	0.658
Be08 Co-15				200	360		22.528	2.019	3.16E-13	2.835	0.110	2.182	8.30E-13	8.039	0.648
Be08 Co-16				150	270		22.153	2.024	4.71E-13	4.302	0.165	3.214	1.21E-12	17.548	0.773
Be08 Co-17				125	225		20.353	2.042	4.84E-13	4.852	0.190	11.552	4.11E-13	23.337	1.002
Be08 Co-18				175	315		21.818	2.029	3.98E-13	3.702	0.131	2.119	1.50E-12	14.542	0.665
Be08 Co-19				100	180		22.464	2.026	8.76E-13	7.895	0.274	13.040	4.71E-13	27.357	1.148
Belle–Roche terrace (*Amblève valley*)															
Be07 BR-20	50.481	5.616	153	600	1380	1.180	46.641	2.040	4.15E-13	1.815	0.037				
Be07 BR-21				550	1265		45.645	2.051	2.42E-13	1.087	0.031				
Be07 BR-22				500	1150		43.727	2.040	3.32E-13	1.548	0.037				
Be07 BR-23				450	1035		44.363	2.043	2.47E-13	1.137	0.033				
Be07 BR-24				400	920		45.887	2.046	1.56E-13	0.695	0.022				
Be07 BR-25				300	690		44.548	2.048	1.12E-13	0.514	0.019				
Be07 BR-26				200	460		46.079	2.041	1.63E-13	0.722	0.025				
Be07 BR-27				150	345		43.691	2.078	3.00E-13	1.429	0.031				
Be07 BR-28				100	230		41.630	2.011	4.41E-13	2.131	0.037				
Be07 BR-29				60	138		42.690	2.050	7.50E-13	3.600	0.061				
Stavelot terrace (*Amblève valley*)															
Be07 St-40	50.396	5.944	305	300	690	1.363	43.210	2.049	2.57E-13	1.221	0.053				
Be07 St-41				250	575		44.422	2.056	7.47E-14	0.346	0.016				
Be07 St-42				200	460		43.329	2.048	9.79E-14	0.463	0.014				
Be07 St-43				150	345		43.207	2.056	3.13E-13	1.490	0.029				
Be07 St-44				100	230		41.459	2.055	4.76E-13	2.362	0.112				
Be07 St-45				50	115		45.287	2.055	9.13E-13	4.143	0.088				
Lodomez terrace (*Amblève valley*)															
Be07 Lo-50	50.391	5.972	307	450	855	1.365	46.938	2.055	4.12E-13	1.805	0.033				
Be07 Lo-51				400	760		46.702	2.024	1.98E-13	0.857	0.021				
Be07 Lo-52				350	665		43.482	2.092	1.11E-13	0.536	0.017				
Be07 Lo-53				300	570		44.266	2.055	2.13E-13	0.988	0.030				
Be07 Lo-54				250	475		45.034	2.038	1.06E-13	0.478	0.019				
Be07 Lo-55				200	380		45.031	2.051	2.31E-13	1.053	0.022				
Be07 Lo-56				165	313.5		45.593	2.047	3.73E-13	1.676	0.040				
Be07 Lo-57				100	190		46.220	2.048	6.82E-13	3.020	0.056				
Be07 Lo-58				50	95		43.482	2.045	1.03E-12	4.836	0.130				

[a] Production rates were scaled following Stone (2000) with a sea level high latitude production rate of (4.5 ± 0.3) at/g/yr.
[b] For each sample, addition of ~100 µl of an in-house 3.10^{-3} g/g ^{9}Be carrier solution.
[c] ^{27}Al concentrations, naturally present in the samples (no carrier), were measured by ICP-OES.

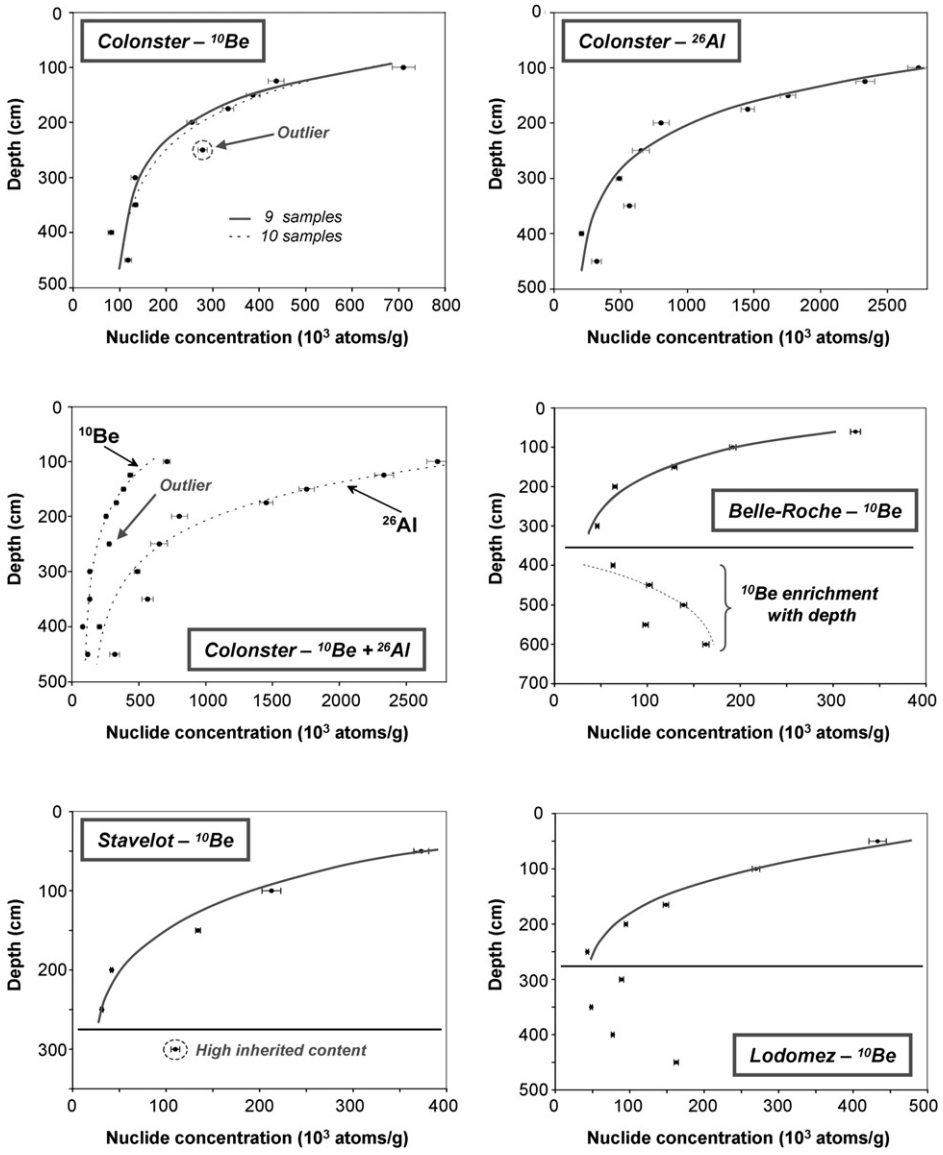

Fig. 4. TCN depth profiles with measured (points) and modeled (curve) concentrations. In the first profile (Colonster ^{10}Be), the outlier removed from the modeling is encircled (Be08-Co14). In the last three profiles (Amblève valley terraces), surface exposure modeling was performed on the basis of the five surface samples (above the horizontal line).

uncertainty, generally taken as the plot area with $\chi^2_i \leq \chi^2_{min} + 1$ (Granger, 2006).

In the Amblève valley, the upper part of the ^{10}Be profiles allowed us to provide unequivocal exposure ages for the three terraces. The best fits assign similar ages of 135 ± 6 and 140 ± 9 ka respectively to the Stavelot and Lodomez terraces. Neither inheritance (assumed identical for all samples of a profile), nor denudation of the alluvial surface is found in these sites. Consequently, both terrace exposure times are very well constrained, as shown by the very small time range of the 1σ confidence interval in the χ^2 distribution of the time-denudation model plots (Fig. 5). Likewise based on the five surface samples, the four-parameter adjustment of the Belle–Roche profile provides an age of 222.5 ± 31 ka for the abandonment of the terrace. It also indicates that the Belle–Roche terrace experienced a denudation rate of 4 m/Ma, corroborating field observations that, at the sampling place, the terrace was no longer in pristine condition, with a clear transverse slope indicative of post-depositional reworking. Owing to this non-zero

Table 2
Modeling results for the Ourthe and Amblève terraces.

Sampled terrace	TCN Used	Data number	Exposure time (ka)	Denudation rate (m/Ma)	Inheritance (katoms/g)	Density (g/cm^3)	χ^2_{min} (median value)
Colonster	^{10}Be	9	390 ± 35	0.5	90	1.86	59.32
	^{26}Al	10	243 ± 10	0	0	1.89	88.42
	^{10}Be/^{26}Al	19	330 ± 30	2	100/0	1.85	259.39
Belle–Roche	^{10}Be	5	222.5 ± 31	4	20	2.3	47.6
Stavelot	^{10}Be	5	135 ± 6	0	0	2.3	266.5
Lodomez	^{10}Be	5	140 ± 9.5	0.1	0	1.9	92.4

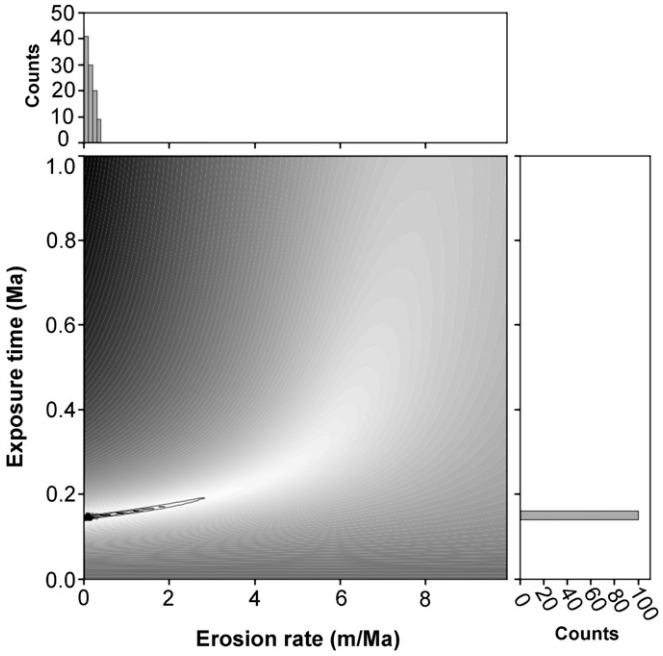

Fig. 5. Diagram of modeled erosion rate and exposure time for the Lodomez terrace deposit. Hundred runs have been performed with ^{10}Be concentrations taken randomly within the analytical error range in order to account for this error. For each run, the χ^2 value associated with every (ε,t) couple is computed, then the median of the 100 χ^2 values is determined for each couple and the solution corresponds to the (ε,t) couple displaying the minimum median value. The diagram displays the median of the 100 χ^2 values computed at each point (from minimum in white to maximum in black) and the final solution (black dot) with 1, 2 and 3σ curves. To the top and right of the diagram, distributions of the best fit ε and t values obtained from the 100 runs are shown.

denudation, the uncertainty on the exposure age is greater than in Stavelot and Lodomez but, as steady–state equilibrium has not yet been reached for this terrace, its exposure time can still be constrained.

In contrary to what is observed in the Amblève terraces, the whole ^{10}Be and ^{26}Al profiles of Colonster are consistent with curves decreasing exponentially with depth, so that all data can be used to determine an exposure age. We modeled separately ^{10}Be and ^{26}Al ages, then, we jointly treated the ^{10}Be and ^{26}Al data (see Table 2). The modeling of the ^{10}Be data set, from which Be08-Co14 (at 250 cm depth) was excluded as an outlier, yields an exposure age of 390 ± 35 ka, a denudation rate of 0.5 ± 0.5 m/Ma and an inheritance of ~90 kat/g. Performing the same modeling with the ^{26}Al data set (no outlier) produces an exposure age of 243 ± 10 ka, no denudation and no inheritance. These results were obtained using the muonic components of the ^{26}Al production rate determined by Heisinger et al. (2002a,b). When modeled jointly, the ^{10}Be and ^{26}Al datasets (with the exception of sample Be08-Co14 for ^{10}Be) yield an exposure age of 330 ± 30 ka, a denudation rate of 2.0 ± 0.5 m/Ma, an inheritance of ~100 kat/g for ^{10}Be and no inheritance for ^{26}Al.

The surprisingly low exposure age obtained for the ^{26}Al data set (with respect to that derived from the ^{10}Be and combined data) may result from using Heisinger et al. (2002a; 2002b) parameters for muon productions. Indeed, the physical parameters reported by Heisinger et al. (2002a; 2002b) are based on laboratory experiments for discrete muon energies and thus may not be directly applicable to the broader energy spectrum present in the natural environment. Heisinger et al. (2002a,b) parameters may consequently overestimate muon productions at depth. Braucher et al. (2003) reached a similar conclusion for ^{10}Be. As the parameters used for ^{10}Be have been determined from measurements in natural samples, the Colonster exposure age of 390 ± 35 ka determined from the ^{10}Be depth profile appears to be most robust and thus will be used next.

4.3. The buried terrace at Romont

The burial of the Romont gravels beneath 3 m of loess indicates a complex history of the deposit and implies additional difficulty in its age determination. The main problem is that no information is available regarding the duration of the burial: the observed loess cover is of Weichselian age, but did the previous glacials cause a similar loess accumulation? Can we make the approximation of a temporally continuous cover above the gravels over several glacial cycles simply because this seems geomorphologically reasonable and to some extent supported by the preservation of pre-Weichselian loess elsewhere in the area?

In any case, the observed exponential decrease of the TCN content with depth in the gravels points to an undisturbed exposure episode. Assuming first that the sample depths were always identical to those presently measured however leads to a modeling impossibility, as the measured TCN concentrations can in no case have been accumulated at such depths. We thus had to include in the modeling an initial episode of surface exposure of the gravels before burial. Under the assumption of a simple episode of exposure followed by continuous burial (Granger et al., 1997), the ^{26}Al/^{10}Be ratio of 3.93 ± 0.47 associated with a ^{10}Be concentration of (654.4 ± 103.9) kat/g obtained for the highest sample within the depth profile yields a burial time of 705 ± 210 ka and a maximum denudation rate before the burial event in the order of 5 m/Ma.

However, as mentioned above, the exponential decreases observed for both ^{10}Be and ^{26}Al lead us to propose a model with a simple exposure episode at the surface free from any loess cover (hereafter called "surface exposure"), followed by a rapid burial and a subsequent exposure under the current 3.1 m thick loess cover (hereafter, "depth exposure") (Fig. 6.A). To fit such a two-step scenario to the data, it has to be considered that the measured concentrations ($C_{\text{meas.}}$) result from the evolution of concentrations acquired (1) in a deposit affected by denudation (ε) during exposition at depths corresponding to sampling depths minus the 3.1 m of the current loess cover (C_1 in Eq. (3), also including the inherited pre-depositional concentrations C_0 of Eq. (2) and 2 during their burial at their sampling depths, with inherited concentrations corresponding then to the pre-burial concentrations C_1. It results from this scenario that six unknown parameters have to be determined simultaneously. These parameters are the exposure duration at "surface" (t_S), the exposure duration at "depth" (t_B), the denudation rate (ε), the inherited concentrations (C_0) for both ^{10}Be and ^{26}Al at the time of deposition, and the density (ρ). This is summarized in Eq. (3) that is a modified Eq. (2) where the inheritance term C_0 has been replaced by Eq. (2) itself (expressed here as C_1):

$$\begin{aligned} C_{\text{meas}} = {} & \frac{P_n}{\frac{\varepsilon}{\Lambda_n}+\lambda}\cdot e^{-\frac{x}{\Lambda_n}}\left[1-\exp\left\{-t_B\left(\frac{\varepsilon}{\Lambda_n}+\lambda\right)\right\}\right] \\ & + \frac{P_{\mu s}}{\frac{\varepsilon}{\Lambda_{\mu s}}+\lambda}\cdot e^{-\frac{x}{\Lambda_{\mu s}}}\left[1-\exp\left\{-t_B\left(\frac{\varepsilon}{\Lambda_{\mu s}}+\lambda\right)\right\}\right] \\ & + \frac{P_{\mu f}}{\frac{\varepsilon}{\Lambda_{\mu f}}+\lambda}\cdot e^{-\frac{x}{\Lambda_{\mu f}}}\left[1-\exp\left\{-t_B\left(\frac{\varepsilon}{\Lambda_{\mu f}}+\lambda\right)\right\}\right] \\ & + C_1\cdot e^{(-\lambda t_B)} \end{aligned} \quad (3)$$

with $C_1 = C_{(x,\ \varepsilon,\ ts)}$ is thus determined using Eq. (2) where X is the sampling depth (x) minus the 3.1 m of the current loess cover and t_S the exposure duration at "surface" as explained above.

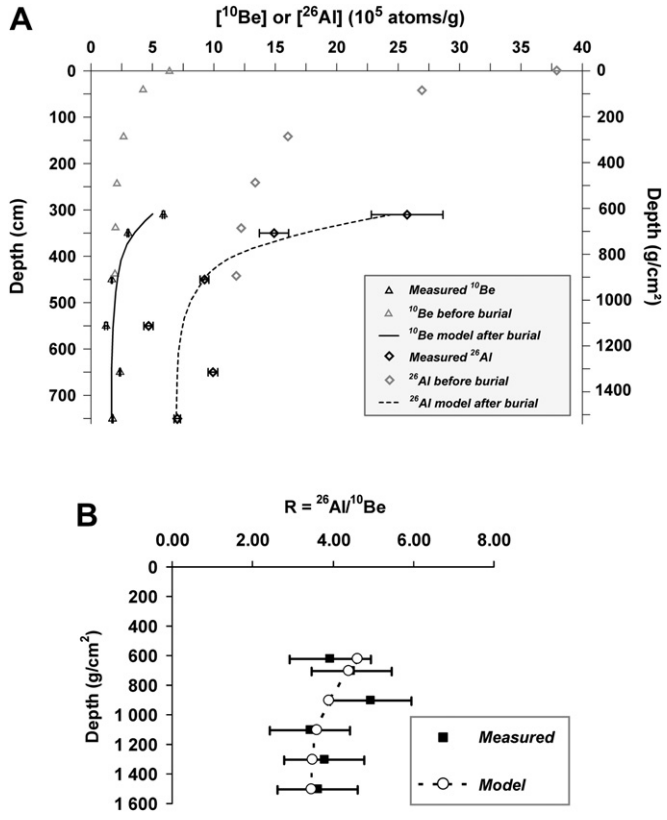

Fig. 6. A. ^{10}Be and ^{26}Al depth profiles for the Romont terrace. B. Measured and modeled ^{26}Al/^{10}Be ratios as a function of depth for the Romont terrace.

Assuming that the denudation rate remained constant all along the exposure history and that it cannot be higher than 5 m/Ma (as determined with the estimation of the burial age from the highest sample within the depth profile), considering also that the ^{26}Al/^{10}Be ratios must be lower than 6.61 (Fig. 6B), this model yields exposure durations at "surface" (t_S) of 100 ± 15 ka and at "depth" (t_B) of 625 ± 120 ka, no denudation and pre-exposure inherited concentrations of 257 and 1700 kat/g for ^{10}Be and ^{26}Al, respectively. Despite the stochastic nature of inheritance, the observed exponential decrease of both ^{10}Be and ^{26}Al concentrations with depth as well as the similarity of the ^{26}Al/^{10}Be ratios most likely imply that the inherited pre-depositional concentrations may reasonably be considered as constant along the profile. Thanks to this modeling procedure, we set the abandonment of the Romont terrace at 725 ± 120 ka (in agreement with the burial age range of 705 ± 210 ka estimated above).

5. Discussion

5.1. Age of the YMT in the lower Meuse

The age assignments of the terrace flight of the Meuse valley in the Liège-Maastricht area are rather confusing. This results from geomorphological reasons, namely the great number of vertically closely spaced terrace (sub)-levels and the probability of large meander cut-off in the area during the middle Pleistocene (Juvigne and Renard, 1992), and also from the diverse interpretations of the few available paleomagnetic data (Felder and Bosch, 1989; Juvigne and Renard, 1992; Van Den Berg, 1996; Van Balen et al., 2000; Westaway, 2002).

Felder and Bosch (1989) identified the Meuse "main terrace" in the Maastricht area as a single level that they called the Sint Pietersberg (SP) terrace. Based on the assumption of a climatic origin of the terraces and a comparison with the Marine Isotopic Stages (MIS), they suggested an age of ~0.7 Ma for this level. In a more complete reconstruction of a flight of 31 terraces, Van Den Berg (1996) subdivided the SP (or main) terrace in three sublevels and assigned them respectively to MIS 26, 22 and 20 (respectively, 0.96, 0.87 and 0.80 Ma). By contrast, relying on new correlations with the Meuse terraces in the Liège area, Van Balen et al. (2000) suggested that the oldest SP sublevel, SP1, dates from 0.72 Ma and that the terrace just below the main terrace complex dates from 0.65 Ma. Recently, still another opinion was given by Westaway (2002), who correlated the three SP sublevels with MIS 22, 20 and 18 (i.e., 0.87, 0.80 and 0.72 Ma). Considering now the few paleomagnetic data collected by Van Den Berg (1996), the main observation concerns the presence of reverse and normal polarities within two sections of the SP2 level, while only normal polarity was found in SP1 and SP3. If reliable, this suggests that the middle SP sublevel would have formed at the Matuyama–Brunhes transition (~0.78 Ma) and that the YMT (corresponding to the SP3 level in the Maastricht area) would be younger, as suggested by Westaway (2002).

Before discussing the meaning of our TCN age at Romont, we need to correlate this terrace element with the terrace flight at Maastricht. Based on altitudinal comparison with the SP sublevels 5 km downstream, the Romont terrace (base at 109 m asl) most probably belongs to SP2 (104.5 m asl). A look upstream towards the subdivided main terrace complex in the Liège area (Juvigne and Renard, 1992) however provides no firm indication to decide whether it is better correlated with the local equivalent of SP2 or SP3.

The TCN age of 725 ± 120 ka at Romont suggests that the terrace belongs to MIS 18. Actually, it indicates that the terrace was abandoned due to incision around the end of MIS 18 and thus was accumulated mainly during this stage. This interpretation not only sheds doubt about the paleomagnetic data in the Maastricht area, but it also makes SP2 (and thus also SP3) younger than the latest estimate of Westaway (2002) and leads to conclusions very similar to those of Felder and Bosch (1989) and Van Balen et al. (2000), suggesting that the SP2-SP3 succession might have developed within a relatively short timespan, perhaps as a complex response to the starting incision wave of the middle Pleistocene. Finally, this age assignment is also remarkably consistent with the most recent views about the Rhine terrace chronology at its passage from the Rhenish shield into the Lower Rhine Embayment, where the UT2/3 and UT4 terrace levels, corresponding respectively to SP2 and SP3, have also been ascribed to MIS 18 and 16 (Boenigk and Frechen, 2006).

5.2. Diachronic post-YMT river incision in the NE Ardennes

The most striking result of this study is undoubtedly the considerable age discrepancy of the YMT level within the three investigated valleys. From the geometric correlation and the geomorphological similarity between the terraces, we actually expected uniform ages at Romont, Colonster and Belle–Roche. In contrast, while the Romont age of 725 ± 120 ka marks the start of the post-YMT incision north of the Ardennes massif, a consistent age decrease is observed when going upstream along the lower Meuse - lower Ourthe - Amblève system. Indeed, the ^{10}Be age of Colonster (390 ± 35 ka) is indisputably more recent than that of Romont and the abandonment of the Belle–Roche terrace around 220 ka obviously evidences that the erosion wave reached this part of the drainage network with considerable further delay. Although the Stavelot and Lodomez terraces, located still farther upstream in the drainage network, probably pertain to the level just below the

YMT, their very young ages (both around 140 ka) also consistently integrate into this scheme.

Our whole data set thus unequivocally establishes that the post-YMT river incision occurred diachronically in NE Ardennes, the erosion wave needing more than half a million years to propagate from the Maastricht area towards the Ardennian headwaters of the Meuse catchment. This contradicts the long-held statement of a climatically driven, simultaneous incision throughout the catchment, which implied that geometrically correlated terrace levels were assumedly everywhere of the same age, and erroneously allowed previous authors to propagate local age information within the drainage network (e.g., Meyer and Stets, 1998).

However, a main characteristic of the Meuse-Ourthe-Amblève system is that it includes rivers of very different size (the Meuse catchment at Liège represents ~20,500 km^2 whereas that of the Amblève is only of 1070 km^2). As the celerity c of a wave of erosion is strongly dependent on the drainage area A (e.g., Whipple and Tucker, 1999), it is thus not surprising to observe delays in the time of terrace abandonment when comparing smaller sub tributaries with the main stem. This is quite different as long as one remains in the same valley, where A and c diminishes slowly, and the propagation of an erosion wave along the whole Ardennian part of the Meuse valley (i.e., ~180 km from Liège, north of the massif, to Charleville, the entrance point of the Meuse in S Ardennes) occurs probably in only a few ka, as suggested notably by the-sudden and widespread change in mineralogy observed in a single Meuse terrace level across the Ardennes after the Mosel capture (Pissart et al., 1997). Therefore, whereas most studies dealing with terrace chronology along the main rivers in the massif (namely the Meuse, the Rhine and the Mosel) remain valid, those involving comparison of the intra-massif tributaries with the terrace system of the major rivers should be seriously questioned (e.g., Meyer and Stets, 1998; Van Balen et al., 2000; Juvigne et al., 2005).

5.3. ^{10}Be enrichment at the base of the Belle–Roche profile: dating the time of floodplain formation vs terrace abandonment

At Belle–Roche, the TCN age of ~220 ka may be compared with a paleontological age estimate of a cave deposit situated ~12 m above the base of the YMT. This deposit comprises a basal layer of gravels of the Amblève overlain by runoff and solifluction products. Based on a rich fauna of macro- and micromammals, the latter were dated as of ~500 ± 70 ka (Cordy et al., 1993), thus implying a slightly older age for the river gravel. Although the two ages are actually not inconsistent, this ~300 ka discrepancy deserves particular consideration, as does also the unusual thickness (~8 m) of the Belle–Roche terrace deposit.

While the age of 220 ka derived from the ^{10}Be data is an estimate of the time of the YMT abandonment, we should recall that, in the modeling, we left aside the data points witnessing an anomalous enrichment in ^{10}Be below 3 m depth (Fig. 4). We suggest that this high ^{10}Be content at depth was acquired during a long-lasting phase of progressive, slow accumulation of river gravel. During the accumulation, the upper part of the deposit was constantly renewed, hampering the *in situ* TCN production, while its deeper part, though less exposed to the cosmic rays, was able to store the produced ^{10}Be. The thickness of the constantly reworked upper part may be inferred from the ~3 m thickness of the present floodplain of the lower Amblève. When the deposit grew, its deep ^{10}Be-accumulating part also progressively thickened. At the final stage, just before the Amblève started to incise its YMT floodplain, the gravel layer below the upper 3 m of transit material had accumulated ^{10}Be in proportion to its residence time in the deposit. When incision began, the upper transit material, which was still devoid of *in situ* produced ^{10}Be, was in turn immobilized in the terrace and started to accumulate ^{10}Be following the usual exponential depth profile. Indeed, the exponential part of the Belle–Roche ^{10}Be curve is 3-m deep, corresponding to the estimated thickness of the transit material. The modeling of the lower, non-exponential part of the ^{10}Be profile yields an accumulation rate of ~25 m/Ma for the river gravel. The age of the deepest sample, located at ~6 m below the ground surface, can be estimated to be on the order of 460 ka (240 ka of progressive burial plus 220 ka of exposition after the abandonment of the terrace). However, the YMT deposit at Belle–Roche is estimated to be a good 8 m thick (Juvigne et al., 2005). Assuming that the accumulation rate remained constant over the time of formation of the whole sequence and taking into account the calculated denudation rate of 4 m/Ma, this would provide a total burial time of ~360 ka, indicating that the terrace began to form at least around 580 ka, and continued up to its time of abandonment at 220 ka. We are thus able to distinguish between the time of formation of the terrace before MIS 14, consistent with the paleontological age of the place and also likely identical to that of its geometric equivalent (SP3) at Romont, and the time of its abandonment, which occurred when the erosion wave finally reached the lower Amblève, ~0.5 Ma ka after it had passed Romont.

6. Conclusion

A main result of our study has been to propose the first absolute age of the Meuse Main Terrace. As the terrace gravels are buried beneath Weichselian loess in the lower Meuse valley at Romont, the use of the highest sample from the studied buried depth profile yields at first glance a burial age of 705 ka with a large associated error range of 210 ka. Using the whole data set of the depth profile, we were however able to refine the age determination, finally obtaining an age of 725 ± 120 ka that links the Romont level to MIS 18. Similar to the age proposed by Felder and Bosch (1989) and Van Balen et al. (2000) on the basis of correlation with the marine isotope stages, this TCN age consequently questions the validity of the paleomagnetic data at Maastricht.

As for the ages we obtained for the same Main Terrace level in the Ardennian valleys, they become younger as they come closer to the headwaters, leading us to another far-reaching conclusion, namely that the abandonment of this terrace was not climatically forced, as generally believed, but occurred diachronically along the drainage network, over the ~0.5 Ma timespan needed by a tectonically induced erosion wave to propagate from the northern margin of the Ardennes towards the heart of the massif. This interpretation is quite consistent with the finding that, at Belle–Roche (and possibly also at Lodomez) in the Amblève valley, a gradual ^{10}Be enrichment in the lower half of the depth profile resulted from a long-lasting accumulation of the terrace gravels. Therefore, if the times when the geometrically correlated Romont and Belle–Roche terraces began to form are fairly consistent, their time of abandonment on the other hand is quite different, depending on the passage of the erosion wave.

These conclusions highlight the potential of cosmogenic nuclides for yielding reliable ages of Middle Pleistocene river terraces. They also underline the need for further such dating in order to better constrain the uplift/incision history of the Ardennes and the Rhenish shield.

Acknowledgements

The authors thank L. Leanni, M. Arnold and G. Aumaître for their respective valuable assistance during chemical treatments and ^{10}Be and ^{26}Al measurements at the ASTER AMS national facility (CEREGE, Aix-en-Provence) which is supported by the INSU/CNRS, the French Ministry of Research and Higher Education, IRD and CEA.

We also thank an anonymous reviewer, Greg Balco and John Gosse for their pertinent reviews and constructive suggestions. They greatly helped to improve the manuscript.

Editorial handling by: R. Grun

References

Antoine, P., 1994. The Somme valley terrace system (Northern France); a model of river response to quaternary climatic variations since 800,000 BP. Terra-Nova 6, 453–464.

Antoine, P., Lautridou, J.-P., Laurent, M., 2000. Long-term fluvial archives in NW France: response of the Seine and Somme rivers to tectonic movements, climatic variations and sea-level changes. Geomorphology 33, 183–207.

Arnold, M., Merchel, S., Bourles, D.L., Braucher, R., Benedetti, L., Finkel, R.C., Aumaître, G., Gottdang, A., Klein, M., 2010. The French accelerator mass spectrometry facility ASTER: improved performance and developments. Nuclear Instruments and Methods in Physics Research B: Beam Interactions with Materials and Atoms 268, 1954–1959.

Boenigk, W., Frechen, M., 2006. The Pliocene and Quaternary fluvial archives of the Rhine system. Quaternary Science Reviews 25, 550–574.

Braucher, R., Brown, E.T., Bourles, D.L., Colin, F., 2003. In situ produced ^{10}Be measurements at great depths: implications for production rates by fast muons. Earth and Planetary Sciences Letters 211, 251–258.

Braucher, R., Del Castillo, P., Siame, L., Hidy, A.J., Bourles, D.L., 2009. Determination of both exposure time and denudation rate from an in situ-produced ^{10}Be depth profile: a mathematical proof of uniqueness. Model sensitivity and applications to natural cases. Quaternary Geochronology 4, 56–67.

Bridgland, D.R., 2000. River terrace systems in north-west Europe: an archive of environmental change, uplift and early human occupation. Quaternary Science Reviews 19, 1293–1303.

Bridgland, D.R., Westaway, R., 2008. Climatically controlled river terrace staircases: a worldwide Quaternary phenomenon. Geomorphology 98, 285–315.

Brocard, G.Y., Van Der Beek, P.A., Bourles, D.L., Siame, L.L., Mugnier, J.-L., 2003. Long-term fluvial incision rates and postglacial river relaxation time in the French Western Alps from ^{10}Be dating of alluvial terraces with assessment of inheritance, soil development and wind ablation effects. Earth and Planetary Science Letters 209, 197–214.

Brown, E.T., Edmond, J.M., Raisbeck, G.M., Yiou, F., Kurz, M.D., Brook, E.J., 1991. Examination of surface exposure ages of Antarctic moraines using in situ produced ^{10}Be and ^{26}Al. Geochimica et Cosmochimica Acta 55, 2269–2283.

Brown, E.T., Bourles, D.L., Colin, F., Raisbeck, G.M., Yiou, F., Desgarceaux, S., 1995. Evidence for muon-induced production of 10Be in near-surface rocks from the Congo. Geophysical Research Letters 22 (6), 703–706.

Brunnacker, K., Boenigk, W., 1983. The Rhine valley between the NeuwiedBasin and the lower Rhenish Embayment. In: Fuchs, K., et al. (Eds.), *Plateau Uplift, the Rhenish Shield - a Case History*. Springer, pp. 62–73.

Chmeleff, J., Von Blanckenburg, F., Kossert, K., Jakob, D., 2010. Determination of the ^{10}Be half-life by multicollector ICP-MS and liquid scintillation counting. Nuclear Instruments and Methods in Physics Research B: Beam Interactions with Materials and Atoms 268, 192–199.

Cordier, S., Harmand, D., Frechen, M., Beiner, M., 2006. Fluvial system response to middle and upper Pleistocene climate change in the Meurthe and Moselle valleys (EasternParis Basin and Rhenish massif). Quaternary Science Reviews 25, 1460–1474.

Cordy, J.M., Bastin, B., Demaret-Fairon, M., EK, C., Geeraerts, R., Groessens-Van Dyck, M.C., Oze, A., Peuchot, R., Quinif, Y., Thorez, J., Ulrix-Closset, M., 1993. La grotte de La Belle-Roche (Sprimont, Province de Liège): un gisement paléontologique et archéologique d'exception au Benelux. Bulletin de l'Académie royale de Belgique, Classe des Sciences 6e (4), 165–186.

Cornet, Y., 1995. L'encaissement des rivières ardennaises au cours du Quaternaire. In: Demoulin, A. (Ed.), L'Ardenne, Essai de Géographie Physique. Département de Géographie Physique et Quaternaire, Université de Liège, pp. 155–177.

Cronus calculator documentation, 2009. hess.ess.washington.edu/math/docs/al_be_v22/AlBe_changes_v22.pdf.

Demoulin, A., 2004. Reconciling geodetic and geological rates of vertical crustal motion in intraplate regions. Earth and Planetary Science Letters 221 (1–4), 91–101.

Demoulin, A., Hallot, E., Rixhon, G., 2009. Amount and controls of the Quaternary denudation in the Ardennes massif (western Europe). Earth Surface Processes and Landforms 34, 1487–1496.

Demoulin, A., Hallot, E., 2009. Shape and amount of the Quaternary uplift of the western Rhenish shield and the Ardennes (western Europe). Tectonophysics 474, 696–708.

Felder W.M. & Bosch P.B., 1989. Geologische kaart van Zuid-Limburg en omgeving 1:50.000, Afzettingen van de Meuse. Rijks Geologische Dienst, Heerlen.

Gosse, J.C., Phillips, F.M., 2001. Terrestrial in situ cosmogenic nuclides: theory and application. Quaternary Science Reviews 20, 1475–1560.

Granger, D.E., 2006. A review of burial dating methods using ^{10}Be and ^{26}Al: in situ produced cosmogenic nuclides and quantification of geological processes. Geological Society of America Special Paper 415, 1–16.

Granger, D.E., Muzikar, P.F., 2001. Dating sediment burial with in situ produced cosmogenic nuclides: theory, techniques, and limitations. Earth and Planetary Science Letters 188, 269–281.

Granger, D.E., Kirchner, J.W., Finkel, R.C., 1997. Quaternary downcutting rate of the New River, Virginia, measured from differential decay of cosmogenic ^{26}Al and ^{10}Be in cave-deposited alluvium. Geology 25 (2), 107–110.

Heisinger, B., Lal, D., Jull, A.J.T., Kubik, P., Ivy-Ochs, S., Neumaier, S., Knie, K., Lazarev, V., Nolte, E., 2002a. Production of selected cosmogenic radionuclides by muons; 1. Fast muons. Earth and Planetary Science Letters 200, 345–355.

Heisinger, B., Lal, D., Jull, A.J.T., Kubik, P., Ivy-Ochs, S., Knie, K., Nolte, E., 2002b. Production of selected cosmogenic radionuclides by muons; 2. Capture of negative muons. Earth and Planetary Science Letters 200, 357–369.

Houtgast, R.F., Van Balen, R.T., Bouwer, L.M., Brand, G.B.M., Brijker, J.M., 2002. Late quaternary activity of the Feldbiss Fault Zone, Roer valley Rift system, the Netherlands, based on displaced fluvial terrace fragments. Tectonophysics 352, 295–315.

Juvigne, E., Renard, F., 1992. Les terrasses de la Meuse de Liège à Maastricht. Annales de la Société Géologique de Belgique 115 (1), 167–186.

Juvigne, E., Cordy, J.-M., Demoulin, A., Geeraerts, R., Hus, J., Renson, V., 2005. Le site archéo-paléontologique de la Belle-Roche (Belgique) dans le cadre de l'évolution géomorphologique de la vallée de l'Amblève inférieure. Geologica Belgica 8 (1–2), 121–133.

Korschinek, G., Bergmaier, A., Faestermann, T., Gerstmann, U.C., Knie, K., Rugel, G., Wallner, A., Dillmann, I., Dollinger, G., Lierse Von Gostomski, C., Kossert, K., Maiti, M., Poutivtsev, M., Remmert, A., 2010. A new value for the half-life of ^{10}Be by Heavy-Ion Elastic Recoil Detection and liquid scintillation counting. Nuclear Instruments and Methods in Physics Research B: Beam Interactions with Materials and Atoms 268, 187–191.

Lal, D., 1991. Cosmic ray labeling of erosion surfaces: in situ nuclide production rates and erosion rates. Earth and Planetary Science Letters 104, 424–439.

Maddy, D., 1997. Uplift driven valley incision and river terrace formation in southern England. Journal of Quaternary Science 12, 539–545.

Mälzer, H., Hein, G., Zippelt, K., 1983. Height changes in the Rhenish massif: determination and analysis. In: Fuchs, K., et al. (Eds.), Plateau Uplift. Springer, pp. 164–176.

Merchel, S., Herpers, U., 1999. An update on radiochemical separation techniques for the determination of long-lived radionuclides via accelerator mass spectrometry. Radiochimica Acta 84, 215–219.

Merchel, S., Bremser, W., 2004. First international ^{26}Al interlaboratory comparison – PartI. Nuclear Instruments and Methods in Physics Research B: Beam Interactions with Materials and Atoms 223–224, 393–400.

Merchel, S., Arnold, M., Aumaître, G., Benedetti, L., Bourles, D.L., Braucher, R., Alfimov, V., Freeman, S.P.H.T., Steier, P., Wallner, A., 2008. Towards more precise ^{10}Be and ^{36}Cl data from measurements at the 10-14 level: influence of sample preparation. Nuclear Instruments and Methods in Physics Research B: Beam Interactions with Materials and Atoms 266, 4921–4926.

Meyer, W., Stets, J., 1998. Junge Tektonik im Rheinischen Schiefergebirge und ihre Quantifizierung. Zeitschrift der Deutschen Geologischen Gesellschaft 149, 359–379.

Nishiizumi, K., Winterer, E.L., Kohl, C.P., Klein, J., Middleton, R., Lal, D., Arnold, J.R., 1989. Cosmic ray production rates of ^{10}Be and ^{26}Al in quartz from glacially polished rocks. Journal of Geophysical Research 94, 17907–17915.

Pissart, A., Harmand, D., Krook, L., 1997. L'évolution du cours de la Meuse de Toul à Maastricht depuis le Miocène: corrélations chronologiques et traces de capture de la Meuse lorraine d'après les minéraux denses. Géographie physique et Quaternaire 51, 267–284.

Ritter, J.R.R., Jordan, M., Christensen, U.R., Achauer, U., 2001. A mantle plume below the Eifel volcanic fields, Germany. Earth and Planetary Science Letters 186 (1), 7–14.

Rixhon, G., Demoulin, A., 2010. Fluvial terraces of the Amblève: a marker of the Quaternary river incision in the NE Ardenne massif (western Europe). Zeitschrift für Geomorphologie 54 (2), 161–180.

Siame, L., Bellier, O., Braucher, R., Sebrier, M., Cushing, M., Bourles, D., Hamelin, B., Baroux, E., De Voogd, B., Raisbecck, G., Yiou, F., 2004. Local erosion rates versus active tectonics: cosmic ray exposure modeling in Provence (south-east France). Earth and Planetary Science Letters 220 (3–4), 345–364.

Stone, J.O., 2000. Air pressure and cosmogenic isotope production. Journal of Geophysical Research 105, 23753–23759.

Van Balen, R.T., Houtgast, R.F., Van Der Wateren, F.M., Vandenberghe, J., Bogaart, P.W., 2000. Sediment budget and tectonic evolution of the Meuse catchment in the Ardennes and the Roer valley Rift system. Global Planetary Change 27, 113–129.

Van Den Berg, M. W., 1996. Fluvial sequences of the Maas, a 10 Ma record of neotectonics and climate change at various timescales. PhD Thesis, Universiteit Wageningen, pp. 181.

Van Den Berg, M., Van Hoof, T., 2001. The Mass terrace sequence at Maastricht, SE Netherlands: evidence for 200m of late Neogene and Quaternary surface uplift. In: Maddy, D., Macklin, M., Woodward, J. (Eds.), River Basin Sediments Systems: Archives of Environmental Change. Balkema, Rotterdam, pp. 45–86.

Vermeesch, P., 2007. CosmoCalc: an Excel add-in for cosmogenic nuclide calculations. Geochemistry, Geophysics, and Geosystems 8. doi:10.1029/2006GC001530 Q08003.

Westaway, R., 2002. Long-term river terrace sequences: evidence for global increases in surface uplift rates in the late pliocene and early middle pleistocene caused by flow in the lower continental crust induced by surface

processes. Netherlands Journal of Geosciences / Geologie en Mijnbouw 81 (3–4), 305–328.
Westaway, R., Bridgland, D., White, M., 2006. The Quaternary uplift history of central southern England: evidence from the terraces of the SolentRiver system and nearby raised beaches. Quaternary Science Reviews 25, 2212–2250.
Whipple, K.X., Tucker, G.E., 1999. Dynamics of the stream-power river incision model: implications for height limits of mountain ranges, landscape response timescales, and research needs. Journal of Geophysical Research 104 (B8), 17661–17674.
Ziegler, P.A., Cloething, S., Van Wees, J.-D., 1995. Dynamics of intra-plate compressional deformation: the alpine foreland and other examples. Tectonophysics 252, 7–59.
Ziegler, P., Dezes, P., 2007. Cenozoic uplift of variscan massifs in the alpine foreland: timing and controlling mechanisms. Global and Planetary Change 58, 237–269.